

Understanding Hydrogen Rich Superconductors: Importance of Effective Mass and Dirty Limit

Andrew L. Cornelius,¹ Keith V. Lawler,² and Ashkan Salamat^{1,2}

¹*Department of Physics & Astronomy, University of Nevada Las Vegas, Las Vegas, Nevada 89154, USA**

²*Nevada Extreme Conditions Laboratory, University of Nevada, Las Vegas, Las Vegas, Nevada 89154, USA*

(Dated: February 10, 2022)

A class of hydrogen-rich (H-rich) systems, consistent with Type II superconductivity, are known to have very high superconducting transition temperatures T_c and upper critical magnetic field B_{c2} values (up to 288 K and 222 T respectively). By looking at all the experimental H-rich superconductors reported to date most are in the dirty limit, with only the highest T_c values being in the crossover to the clean regime. In this framework, there is a clear understanding of some previous unexplained behaviors: (1) A maximum in B_{c2} as a function of T_c ; (2) a clear change in slope in T_c as a function of pressure in CSH; (3) in zero magnetic field the width of the superconducting transition decreasing with increasing T_c ; and (4) in applied magnetic field the slope of the superconducting width versus field decreasing with increasing T_c . Ginzburg-Landau-Abrikosov-Gorkov (GLAG) theory is used to explain all four of these effects within a framework where increasing T_c is related to increases in both the electron effective mass and scattering length.

I. INTRODUCTION

The route to ambient conditions superconductivity will most likely be achieved from a class of H-rich systems that behave as hydrogen dominant alloys, mimicking metallic hydrogen but at significantly more modest densities.^{1,2} The first report of room temperature superconductivity by Snider *et al.*³ in carbonaceous sulfur hydride (CSH) was measured at 288 K and 268 GPa. Their electrical transport measurements revealed a very sharp transition from the normal to zero-resistance state as a function of both T_c and magnetic field, especially in relation to previous reports on other Type-II superconductors YBCO⁴ and MgB₂ (see Table II). The relative superconducting transition width, $\Delta T_c/T_c$, of CSH decreases in both zero and applied magnetic fields with increasing T_c . Understanding the limits in which these H-rich superconductors lie is key to understanding their properties including the transition widths.

There are many ways that the original Ginzburg-Landau equations⁵ have been expanded by the ideas of Abrikosov-Gorkov (GLAG)⁶ to include microscopic theory, discussed here using the notation of Schmidt.⁷ In cgs units, the difference in free energy between the superconducting and normal state is $G_s - G_n = G_{pair} + G_K + G_H$, where G_{pair} is the condensation energy of the Cooper pairs, G_K is the kinetic energy of the electrons and G_H is the energy due to magnetic field expulsion. In terms of the superconducting wave function Ψ which is the order parameter:

$$G_{pair} = \alpha |t| |\Psi|^2 + \frac{\beta}{2} |\Psi|^4. \quad (1)$$

Here $t = 1 - T/T_c$ is the reduced temperature that goes from $1 \rightarrow 0$ for temperatures below the critical superconducting transition temperature, T_c .

An important parameter is the coherence length, ξ , which is the extent of the wavefunction Ψ . It is also related to the s-wave BCS superconducting Cooper pair

size, and it is the range of the superconducting vortex core in the mixed region in a magnetic field. For consistency, the notation for the given GLAG parameters are their zero temperature values, and their temperature dependence will be given by multiplying these terms by the appropriate quantity as done in Equation 1. Typically, applications of this theory are given in either the clean or dirty limit. In the clean limit $\xi = \xi_{GL}$. However, in the dirty limit where the electron mean free scattering length ℓ is much smaller than ξ_{GL} , one needs to use $\xi = (\ell \xi_{GL})^{1/2}$. There is very little discussion in the literature about the use of these equations in the crossover region between clean and dirty. To bridge the regions, one should use the equation $\xi^2 = \xi_{AV} \xi_{GL}$ where $1/\xi_{AV} = 1/\ell + 1/\xi_{GL}$. Another important parameter is the upper critical field where a magnetic field is no longer expelled from the superconductor, $B_{c2} = \Phi_0/2\pi\xi^2$ where Φ_0 is the flux quantum $hc/2e$. As B_{c2} is a measurable quantity, it is used to experimentally determine ξ , though it is often incorrectly reported in the literature as ξ_{GL} implying the clean limit. In typical experimental units, the relationship between ξ and B_{c2} is

$$\xi (nm) = \frac{17.9}{\sqrt{B_{c2} (T)}}. \quad (2)$$

Moving from the dirty to the clean limit has a profound impact on the superconducting parameters of a system. A recent survey of results within the GLAG model on A15 superconducting Nb_{1- β} Sn _{β} ($0.18 < \beta < 0.26$) materials display this impact.⁸ At $\beta=0.18$ Nb_{1- β} Sn _{β} is clearly in the dirty limit ($\ell \gg \xi_{GL}$). As β is increased, linear behavior is observed in the electron effective mass m^* both from fits to models to obtain experimental T_c values and electronic Sommerfeld coefficient from heat capacity measurements.⁹ Figure 1 shows how the various GLAG parameters vary as one increases m^* by increasing τ . It is important to note that $m^* \propto \beta \propto T_c$, so τ can represent either m^*/m_0^* , β/β_0 or T_c/T_{c0} as the dependent dimen-

sionless variable with an appropriate choice of a reference point.

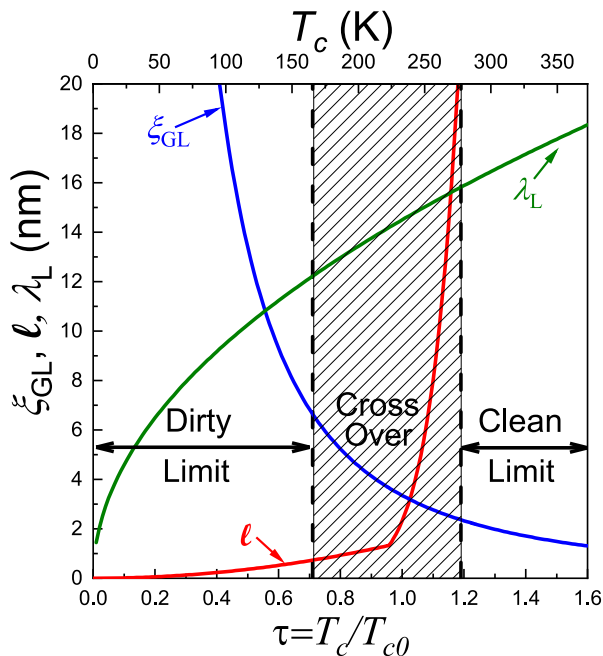


FIG. 1. Various physical parameters from the Ginzburg-Landau-Abrikosov-Gorkov (GLAG) theory applied to H-rich superconductors as a function of superconducting transition temperature T_c (raw value on top x-axis and normalized on the bottom x-axis). ξ_{GL} is the coherence length in the GLAG model in the clean limit. l is the mean electron scattering length. λ_L is the Landau magnetic field penetration depth.

Over the entire range ξ_{GL} and the London penetration depth, λ_L , are assumed to follow their expected GLAG τ^n behavior with $n = -2$ and $+1/2$ respectively. The actual penetration depth can be found using λ_L in the appropriate clean/dirty limit. Initially l increases in a steady power law $l \sim \tau^n$ manner. As l and ξ_{GL} become nearly equal, a superconductor is in the crossover region between the dirty and clean limits, where one must use ξ_{AV} rather than just l (dirty) or ξ_{GL} (clean). Further moving to the right in Figure 1 leads to a much steeper increase in the observed l deduced from B_{c2} and electric transport measurements. The behavior depicted in Figure 1 has implications for many measurable quantities. One is when $l \sim \xi_{GL}$, the value B_{c2} can be found to have a maximum corresponding to a minimum in ξ per Equation 2. Figure 2 shows a plot of B_{c2} normalized by its maximum value plotted versus $\tau = \beta/\beta_0$ to highlight this maximal value for B_{c2} .

For H-rich materials, it is necessary to orient them within the framework of Figure 1. For our analysis of H-rich superconductors, B_{c2} is calculated using the Werthamer-Helfand-Hohenberg (WHH) formalism for consistency. Thus, the published values employed in this analysis are used directly if they were calculated in the WHH formalism, if not they are estimated us-

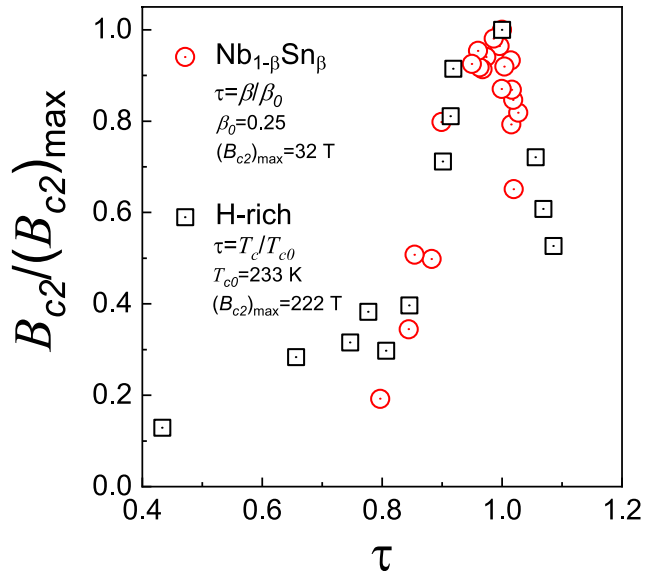


FIG. 2. The upper critical magnetic field B_{c2} versus normalized control parameter τ for A15 $\text{Nb}_{1-\beta}\text{Sn}_\beta$ and H-rich materials. The upper critical magnetic field B_{c2} is normalized by its maximum value chosen to be at $\tau = 1$. $\tau = \beta/\beta_0$ for $\text{Nb}_{1-\beta}\text{Sn}_\beta$ and T_c/T_{c0} for H-rich superconductors.

ing the published data and the WHH equation, $B_{c2} = -0.69 T_c B_{c2}'$ where B_{c2}' is the temperature derivative of B_{c2} at T_c . One difficulty fitting H-rich superconductors to the GLAG model is that all of the measurements are done at very high pressures in a diamond anvil cell (DAC) limiting the number of experimental probes. While the A15 compounds have the advantage of access to the full suite of thermodynamic measurements at ambient pressure, most H-rich measurements in the DAC are electrical transport. While B_{c2} and sometimes l can be extracted from these measurements, other quantities are elusive.

A recent work determining the GLAG parameters for two H-rich superconductors, H_3S and LaH_{10} with T_c values near $T_{c0}=233$ K were able to perform quantifiable magnetic measurements in a DAC leading to a measurement of the Ginzburg-Landau parameter κ that is used to divide Type-I and Type-II superconductors with $\kappa^2 > 1/2$ leading to Type-II superconductivity. κ is the ratio of the London penetration depth λ_L to ξ_{AV} . Table I shows a summary of the results. These results are for two Type-II superconductors with large B_{c2} values near the B_{c2} maximum and lie in the crossover region where $l \sim \xi_{GL}$, which is exactly the case for both materials. The London penetration depth λ_L was taken as the midpoint of the range of values estimated for LaH_{10} in Table I. The clean limit is found where $l \gg \xi_{GL}$ and $l \sim \lambda_L$.

In the H-rich superconductors, like the A15 materials, $m^* \sim T_c$. Figure 2 shows B_{c2} for the H-rich superconductors normalized by its maximum value plotted versus

T_c/T_{c0} for all of the high field data on different H-rich superconductors (where the 0 reference point is chosen as the value where B_{c2} reaches its maximum). The data are in Table III. The overlap is striking and gives strong evidence that Figure 1 should indeed be applicable to the H-rich superconductors. This implies that many of the H-rich superconductors will lie in the dirty region ($\ell \ll \xi_{GL}$) and that the maximum of B_{c2} occurs in a cross over region between the dirty and clean limits.

For CSH, B_{c2} decreases as T_c increases in contrast to lower T_c H-rich systems leading to a maximum in B_{c2} as a function of T_c . This maximum can be explained by a crossover from the dirty to clean regime akin to what is represented in Figure 1. The scenario with CSH is very similar to that observed in $A_{15}Nb_{1-\beta}Sn_{\beta}$ where a change in stoichiometry, rather than pressure, leads to many of the same results.⁸ Herein, we will explain that the decreasing superconducting transition width of CSH is what is expected over the entire the dirty regime, and set forth an explanation for the transition width in H-rich conductors in terms of GLAG theory. Likewise, we will demonstrate that moving into the crossover regime explains the change in the slope of the pressure dependent measured T_c values for CSH. Lastly, we will rationalize the changes in field dependent transition width in CSH and other H-rich superconductors in this context.

A. Moving Towards the Dirty Limit in the H-rich Materials

To continue the analysis, ℓ and ξ_{GL} will be plotted on log-log plots to look for general τ^n dependence over wide ranges representative of Figure 1. This is obviously going to be an overly simplistic view. For example while the actual value of T_c versus $m^* = 1 + \lambda_{e-p}$ for different theories are not linear, it is close enough for general scaling arguments (λ_{e-p} is the electron-phonon coupling).¹⁰ These parameters are: $T_c/T_{c0} = \tau$, $\xi_{GL}/(\xi_{GL})_0 = \tau^{-2}$, $\lambda_{\ell}/\lambda_{L0} = \tau^{1/2}$ and $\rho_n/\rho_{n0} = (\ell/\ell_0)^{-1} = \tau^n$.¹¹ Note that there is no m^* dependence on ℓ which needs to be determined by experiment.

H₃S is the natural continuation point as $R(T)$ data exists for a large region $T_c < T_{c0}$ where one moves entirely to the dirty limit.¹² Finding the dependence of ℓ/ℓ_0 is then critical for determining both the dependence of the GLAG parameters comparing to Figure 1 and how the superconducting transition width will depend on τ . One of the first things that stands out is the normal state resistance decreases dramatically with increasing pressure while T_c increases (see inset of Figure 3). This implies that ℓ increases with T_c . To obtain ℓ one must know the conduction electron density n and the sample thickness t . With the high pressure values being approximately $n = 8.4 \times 10^{22} \text{ cm}^{-3}$ and $t = 2 \mu\text{m}$ respectively,^{12,13} ℓ can be estimated from resistance measurements by the equa-

tion:

$$\ell(nm) = \frac{1.27 \times 10^4 \left(n^{-\frac{2}{3}}\right) t}{\rho_{\Omega-cm}} = \frac{0.235}{R_{\Omega}} \quad (3)$$

For consistency and simplicity, the value of R will be taken just above T_c introducing some uncertainty but typically is small related to other effects. The values of R above T_c , $R(T_c)$, is plotted versus T_c in the Figure 2 inset. Note that no pressure dependence is used for the n and t values. The uncertainty in the absolute value of ℓ is around 50%. This will not change the final discussion (namely the power law dependence of physical properties will be identical) of results, and the relative change uncertainty will probably lie mostly in the aforementioned pressure dependent values of n and t which should be small at very high pressures. The values of ℓ determined from Equation 3 using the $R(T_c)$ data are shown in Figure 3 with ℓ increasing as $\tau^{1.89 \pm 0.13}$.

The values of ξ_{GL} shown in Figure 3 were obtained from the equation $\xi = \sqrt{\ell \xi_{GL}}$. The value of ξ was estimated from B_{c2} measurements on H₃S with a fit to the data for $\tau < 0.8$ gives $\xi = 1.95\tau^{-0.31}$. The value of ξ_{GL} are found to decrease at a rate of $\tau^{-2.18 \pm 0.10}$. The exponent found for ξ_{GL} is remarkably close to the expected -2 value giving credibility to the GLAG formalism used. The data look similar to the expected scenario laid out in Figure 1. Notably, the extrapolated values of ℓ and ξ_{GL} become equal for τ slightly greater than 1. To estimate how close the data lie to the crossover region, the largest temperature where ℓ is determined here for H₃S is $\tau = 0.64$ where $\xi = 0.89\ell$, is right at the crossover region defined here as going from $\xi_{AV} = 0.9\ell$ on the dirty side and $\xi_{AV} = 0.9\xi_{GL}$ on the clean side.

B. Looking at the Crossover Region

Moving on to $\tau > 0.6$ will put a H-rich superconductor into the crossover region. For simplicity and to stay within the ideas of the GLAG model, the exponent for ξ_{GL} will be fixed at -2. Fitting the data gives $\xi_{GL} = 3.35\tau^{-2}$ which will be used over the entire range of τ values. Likewise, fixing the ℓ exponent at 2 gives the fit given $\ell = 1.45\tau^2$.

Another way to obtain the electron mean free path will be to look at the B_{c2} data. Recall B_{c2} gives the value of $\xi = (\xi_{AV}\xi_{GL})^{1/2}$ where $1/\xi_{AV} = 1/\ell + 1/\xi_{GL}$. Figure 4 shows the extrapolated fits for ξ_{GL} and ℓ along with the experimental calculation of ℓ from resistance (Fig. 3) including the two points from transport measurements in Table I and B_{c2} measurements. The values of ℓ from the B_{c2} data qualitatively track the resistance data. The main result of Figure 4 is the sharp increase of ℓ that starts in the region where B_{c2} reaches a maximum. Fitting all of the data in Figure 4 for $\tau > 1$ gives a τ^{13} dependence. The τ^2 fit to ℓ region is extended up until

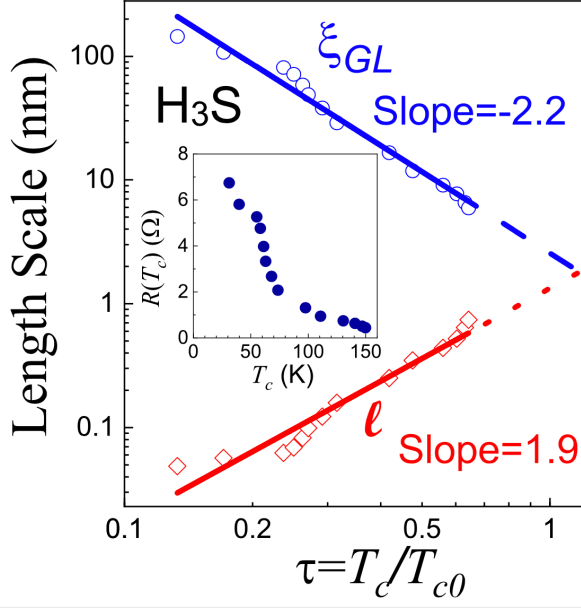


FIG. 3. Calculated values of the mean free electron path ℓ and Ginzburg-Landau coherence length ξ_{GL} from H_3S data. The inset shows the value of the resistance just above T_c , $R(T_c)$ versus T_c .¹²

its intersection with the τ^{13} line which occurs at $\ell=1.34$ nm. This gives $\ell = 2.23\tau^{13}$ nm for $\tau > 0.96$. At $\tau=0.96$, $\xi_{GL}=4.64$ nm which is still larger than ℓ . However, a slight increase in τ leads to a large increase in ℓ and $\ell = \xi_{GL}$ at $\tau=1.03$. The numeric values displayed in Figure 1 have all been calculated and will be used for the following discussion.

Figure 5 shows the overall dependence of ℓ and ξ_{GL} normalized by the ξ_{AV} values as a function of τ . The two values reach their 0.5 values, where they are equal, at $\tau = 1.025$. Recall that the clean limit corresponds to $\xi_{AV}=\xi_{GL}$ while the dirty limit gives $\xi_{AV}=\ell$. While somewhat arbitrary, if $\xi_{AV}/\ell=0.9$ and $\xi_{AV}/\xi_{GL}=0.9$ are chosen for the dirty and clean limits, the crossover region extends from $0.71 < \tau < 1.19$. This gives quantitative values for the crossover region as also shown in Figure 1 (showed by the hatched region in both figures).

Looking at the GLAG theory applied to BCS,⁷ T_c in the dirty limit, takes the form $(T_c)_{dirty} = \alpha\tau^n \times (\xi_{GL}\ell)^{-1/3}$, where the τ^n dependence is due to physical terms like the effective mass and the density of states at the Fermi level and α is a constant. α is slightly different for the clean and dirty limits but will be assumed to be the same for discussion. The product of $\xi_{GL}\ell$ in the dirty limit is independent of T_c so $(T_c)_{dirty} = \alpha\tau^n$ meaning that $n = 1$. The relationship between the dirty and clean limits can be written as $(T_c)_{clean}/(T_c)_{dirty} = (\ell/\xi_{GL})^{+1/3}$ which leads to the crossover approximation of $T_c = T_{c0}\alpha\tau(\xi_{AV}/\xi_{GL})^{+1/3}$ so T_c will no longer be directly proportional to τ due to the

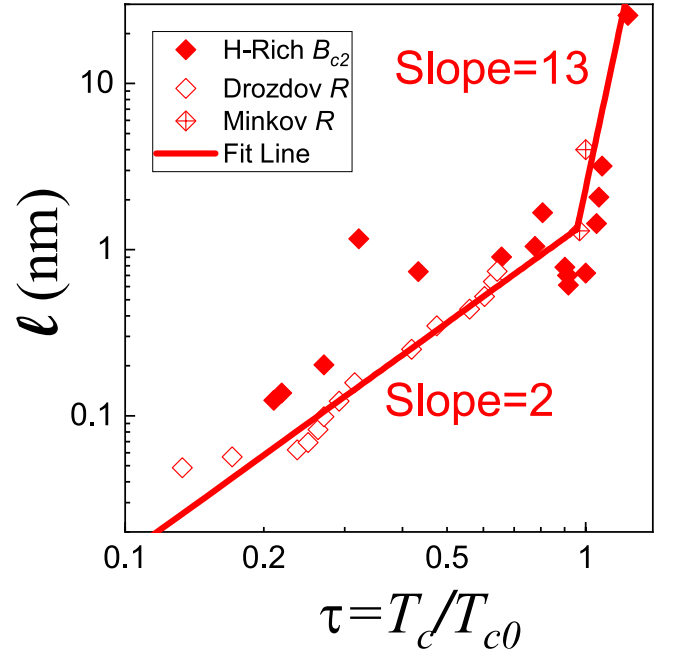


FIG. 4. Mean free electron path for H-rich superconductors as a function of T_c/T_{c0} . This includes resistance data from Figure 3 and Table II (2 points only). Calculated values of the mean free electron path ℓ , using the B_{c2} data (as outlined in text) for all H-rich materials. The sharp upturn is fit using all points in the plot for $T_c/T_{c0} \geq 0.96$.

τ dependence of the ξ terms not cancelling each other.

Turning to the CSH data of Snider *et al.*³, the $T_c(P)$ behavior shows a clear break in slope at high pressure around $T_c/T_{c0}=0.96$ where ℓ drastically changes slope. The data for CSH lie almost entirely in the crossover region and give a good opportunity to test the application of GLAG parameters in this region where the $T_c \sim m^*$ scaling will begin to break down. Looking back to the analysis of De Silva, pressure was used as the driving force to increase m^* and therefore T_c . This was done by fitting $T_c/T_{c0} = 10^{K\Delta P} = \tau_P$ (De Silva used $e^{K\Delta P}$ but log base 10 is used here to keep analysis consistent) where K is a constant. $\Delta P = P - P_0$ where P_0 is the pressure where $T_c=T_{c0}=233$ K, the temperature the hydrides all appear to aggregate around as seen in Figure 2. The subscript P here is for pressure to not confuse with the scaling definition that $\tau \equiv T_c/T_{c0}$. Note that $\tau \sim \tau_P$ in the dirty region, but while τ_P should continue to smoothly increase with pressure, the behavior of τ should be more complicated. Fitting the data from $T_c/T_{c0}=0.69$ to 0.85 which is on the dirty side of the crossover limit (and well before ℓ has the large increase) gives $K=0.00173$ GPa⁻¹. A plot T_c versus τ_P should have a slope of $T_{c0}C_0(\xi_{AV}/\xi_{GL})^{+1/3}$ where α is the only fitting parameter. Using the empirical values from Figure 5, the best fit occurs using $\alpha=0.70$. Figure 6 shows CSH data of Snider along with this fit over an extended range of τ_P . The fit clearly models the data for all τ_P values

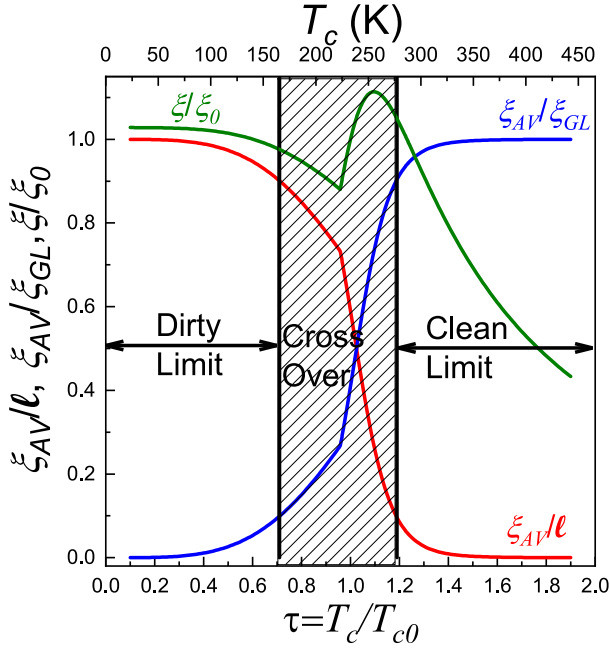


FIG. 5. Plot of ξ_{AV}/ℓ and ξ_{AV}/ξ_{GL} as a function of $\tau = T_c/T_{c0}$ for the aggregate H-rich system data. ℓ , ξ_{AV} , and ξ_{GL} are the electron mean scattering length, average coherence length, and Ginzburg-Landau correlation length. The average coherence length is given by $1/\xi_{AV} = 1/\ell + 1/\xi_{GL}$. The dirty limit ($\ell \ll \xi_{GL}$) here is defined as $\xi_{AV}/\ell \leq 0.9$. The clean limit ($\ell \gg \xi_{GL}$) here is defined as $\xi_{AV}/\xi_{GL} \geq 0.9$. The cross over region is the area between the clean and dirty limits. Note that T_{c0} , the superconducting transition temperature corresponding to the maximum in B_{c2} value clearly lies within the crossover region.

including the change in slope of the T_c data due to the sharp increase in ℓ in this region. $\tau_P = 1.2$ is just short of the clean region, and by $\tau_P = 1.3$ extrapolations will give the expected $\tau_P^{7/3}$ clean limit behavior.

C. Understanding the Superconducting Transition Width

From the GLAG theory, all thermodynamic measurements should exhibit noticeable variations within a temperature range where fluctuations of the order parameter exist. This will occur at the point in zero field where the extent of the wavefunction from the G_{pair} term and wavefunction fluctuations from the G_K term equal each other known as the Ginzburg criterion.¹⁴ This criterion yields the dimensionless Ginzburg or Ginzburg-Levanyuk (not Ginzburg-Landau) number Gi_{clean} for an isotropic 3D superconductor in the clean limit given by:

$$Gi_{clean} = \frac{1}{2} \left[\frac{kT_c}{B_c^2 \xi_{GL}^3} \right]^2 \quad (4)$$

Moving away from the clean limit and taking the re-

sult of Ferrell and Schmidt,¹⁵ the dirty limit value of the Ginzburg-Levanyuk number Gi_{dirty} as:

$$Gi_{dirty} \approx \left[\frac{\xi_{GL}}{\ell} \right]^2 \sqrt{Gi_{clean}} \quad (5)$$

The value of Gi physically gives the temperature range GiT_c near T_c where fluctuations of the order parameter, and therefore to large changes in thermodynamic measurements, are observed. The transition width ΔT_c should be comparable to GiT_c . Rewriting gives $Gi = \Delta T_c/T_c$. While experimental Gi values can be as low as 10^{-13} in clean Type-I 3D superconductors it is common for Type-II anisotropic superconductors to be in the 10^{-2} range as seen in MgB_2 and YBCO.¹⁴

The superconducting transition widths decrease for increasing T_c in the H-rich superconductors in contrast to what is expected, and observed, in superconductors in the clean limit. The τ dependence of Gi in the clean limit is given by:

$$\begin{aligned} \frac{Gi_{clean}}{(Gi_{clean})_0} &= \frac{\Delta T_c/T_c}{(\Delta T_c/T_c)_0} \\ &= \left[\frac{T_c/(T_c)_0}{(B_c/(B_c)_0)^2 (\xi_{GL}/(\xi_{GL})_0)^3} \right]^2 \\ &= \left[\frac{\tau}{(\tau)^2 (\tau^{-2})^3} \right]^2 \\ &= \tau^{10} \end{aligned} \quad (6)$$

The τ dependence for the GLAG parameters here is taken from De Silva.¹¹ This would lead to the conclusion that the superconducting transition increases rapidly

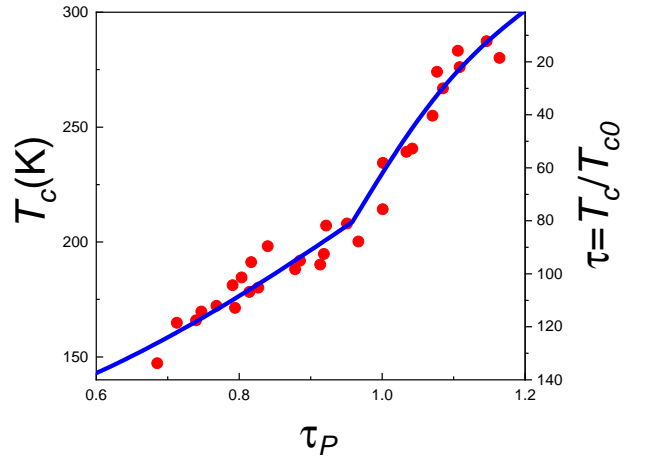


FIG. 6. Superconducting transition temperature as a function of τ_P for carbonaceous sulfur hydride CSH. Data points come from Snider *et al.*³. $\log \tau_P = K \Delta P$ where K is a constant and $\Delta P = P - P_0$ with P_0 chosen as the pressure where $T_{c0} = 233$ K is observed. In the dirty limit $\tau_P \propto \tau$. The line in the figure is a fit using the GLAG theory in the crossover region as discussed in text.

with T_c and effective mass as claimed by Hirsch and Marsiglio.¹⁶ Moving to the dirty limit, using the results from Figure 1, Gi is:

$$\begin{aligned} \frac{Gi_{\text{dirty}}}{(Gi_{\text{dirty}})_0} &= \left[\frac{\xi_{GL}/(\xi_{GL})_0}{\ell/\ell_0} \right]^2 \sqrt{\frac{Gi_{\text{clean}}}{(Gi_{\text{clean}})_0}} \\ &= \left[\frac{\tau^{-2.1}}{\tau^{+1.9}} \right]^2 \sqrt{\tau^{10}} \\ &= \tau^{-3} \end{aligned} \quad (7)$$

In the dirty limit this means that the superconducting transition will narrow with increasing T_c as observed experimentally in heat capacity measurements on $\text{Nb}_{1-\beta}\text{Sn}_\beta$ samples.⁹ For systems between the clean and dirty limits, the crossover region form Gi_{cross} needs to be used where ℓ is replaced by ξ_{AV} . To further look at this scenario an examination of the transitions for all of the H-rich materials needs to be done. There is obviously going to be a great variation in the normal state zero temperature resistance as well as the zero field ΔT_c due to impurities, grain boundaries, disorder, pressure gradients, inhomogeneity and anisotropy to name just a few of many effects. To consistently examine literature values of ΔT_c , the 75%-50% range of the maximum of all the selected normalized $R(T)$ data are used to exclude the broadening that often occurs at $T_c(\text{onset})$ and $T_c(R=0)$ due to multiple effects. This will obviously be a lower bound for the value of ΔT_c , but this best exemplifies the majority phase (ideal) superconducting state. Also, many H-rich samples exhibit a 2 (or more) step transition at low fields that merge into a single transition that is related to the T_c onset phase. Tinkham pointed out that the equations for the resistivity transition broadening do not depend on the range of temperature used as long as the range used is consistent.⁴

The sharpest superconducting transition for a material will be given by the appropriate value of Gi . However, few systems will meet this ideal criteria. In reality, $\Delta T_c/T_c$ should go from Gi to $Gi + \sum(\Delta T_c/T_c)$ where the sum encompasses terms due to a number of factors (inhomogeneity/impurities, surface effects, anisotropy, thermal gradients, etc.). Table II shows numerous measurements on MgB_2 samples. While this is not a complete list, samples including bulk and films are included that display widely varying amounts of strain (including mechanically by ball milling) and impurities. These range of conditions should be a good starting point when comparing to the range of stress states in the H-rich materials. From the measured values in Table II, $(\Delta T_c/T_c)_{\text{min}}=0.0040$. Compared to this minimum value, the largest broadening is just over 65 times larger.

Due to the great variation of the number of published high pressure data sets, criteria for choosing which data to analyze needs to be established. For those reports showing three or fewer $R(T)$ curves, all are analyzed. For those with more than three, the highest, lowest, and sharpest T_c curves are analyzed. Also, any additional

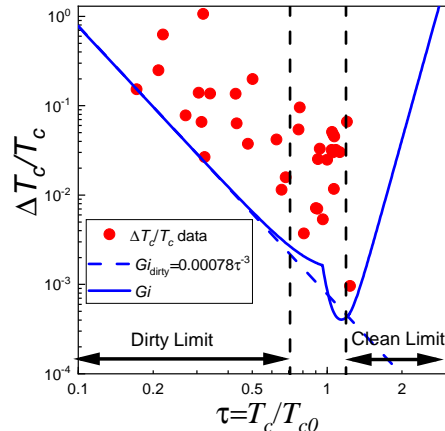


FIG. 7. Values of $\Delta T_c/T_c$ for H-rich superconductors on a log-log plot. The dashed (solid) line are the Ginzburg-Levanyuk numbers Gi in the dirty (cross over) regions that represent the minimum possible $\Delta T_c/T_c$ as a function of $\Delta T_c/T_{c0}$. The experimental values are all given in Table III. (inset) Experimental values of $\Delta T_c/T_c$ divided by the Gi_{cross} line in Figure 7. This give a range of superconducting widths as a function of $\Delta T_c/T_{c0}$. Note that more or less dependent of T_c the range of transition widths is consistent with a span around a factor of 60 which is very close to the factor of 65 found for MgB_2 values in Table II.

$R(T)$ measurements that include magnetic field data will be added and all results analyzed are given in Supplemental Table III. The broadening ($\Delta T_c/T_c$) versus T_c in H-rich materials is shown in Figure 7 on a log-log plot for all known H-rich superconductors. Looking at Figure 7, one can immediately see the trend that the transitions narrow with increasing T_c values. The scatter at fixed values of τ is due to multiple already mentioned factors. The dashed line has the slope of τ^{-3} estimated from Equation 7 that goes through a single point for $\tau < 0.65$ (this would correspond to the sharpest rescaled transition within the dirty limit). The solid line shows how Gi should scale over the entire τ range using the Gi_{cross} approximations from both limits. The two curves split very near 0.71 which is the end of the dirty limit and the start of the crossover region. Also Gi_{cross} starts to increase dramatically as one move to the clean limit and gives the expected clean behavior that Gi_C increases sharply with T_c .

Figure 8 shows the data in Figure 7 rescaled by the Gi line from Figure 7. The range from minimum to maximum widths at all values of τ is very similar to the value of 65 for MgB_2 . The fact that in the dirty limit the sharpest transitions scale as expected (get narrower as τ^{-3}) and the spread in transition widths from smallest to largest is on the order of the range in values for MgB_2 naturally leads to the conclusion that the transition width behavior is far from anomalous and would be expected *a priori* if starting all scaling from Figure 1.

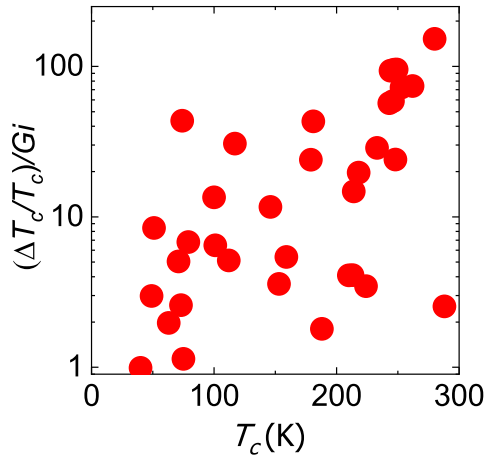


FIG. 8. Experimental values of $\Delta T_c/T_{c0}$ divided by the G_i line in Figure 7. This give a range of superconducting widths as a function of T_c . Note that more or less independent of T_c the range of transition widths is consistent with a span around a factor of 60 which is very close to the factor of 65 found for MgB_2 values in Table II.

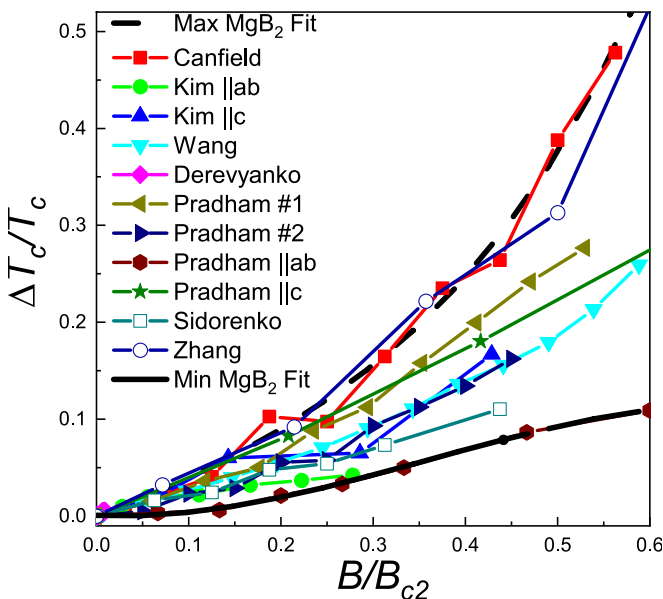


FIG. 9. Compilation of numerous magnetic field broadening $(\Delta T_c/T_{c0})_B$ values for MgB_2 as a function of normalized magnetic field B/B_{c2} . There are numerous single crystal, polycrystalline and film results. The references for each dataset are given in Table 1.

D. Broadening of Superconducting Transition in Applied Magnetic Field

In applied magnetic fields superconducting transitions continue to broaden from their zero field value. Tinkham calculated that this magnetic field broadening should depend on $B^{2/3}$ in agreement with many experimen-

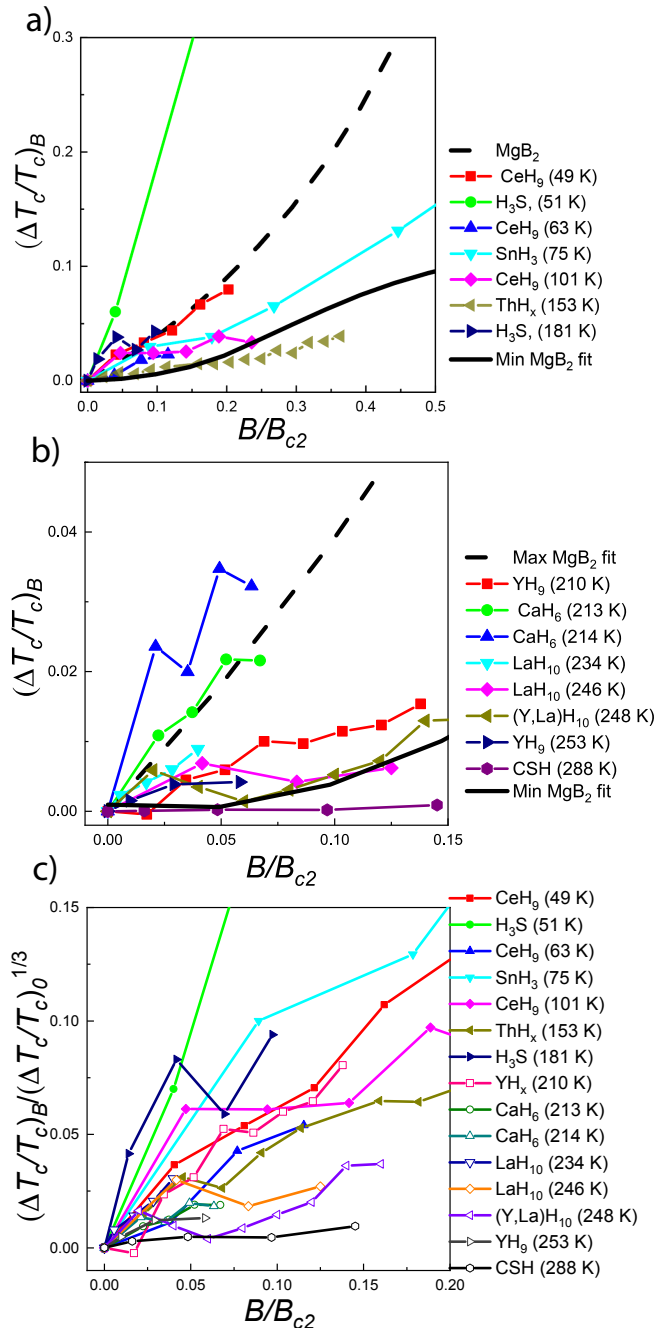


FIG. 10. Values of $(\Delta T_c/T_c)_B$ for H-rich superconductors in applied magnetic field. The raw values for $T_c < 200$ K (a) and $T_c > 200$ K (b) are plotted along with the minimum and maximum experimental values of MgB_2 from Figure 9. (c) The superconducting width rescaled by a factor of $((\Delta T_c/T_{c0})_0)^{1/3}$ which is the cube root of the zero field broadening.

tal results.⁴ This result also follows from GLAG theory (Equation 1) as the addition of the G_{pair} term in applied fields requires an extended temperature range for the mean field approximation to be valid. This leads to

a field induced broadening of

$$(\Delta T_c/T_c)_B = (Gi)^{1/3}(B/B_{c2})^{2/3}, \quad (8)$$

where Gi is the zero-field Ginzburg number.¹⁷ As with zero field transition widths there are many factor that will increase $(\Delta T_c/T_c)_B$ from its minimum value in Equation 8 using Gi . This includes not only the conditions mentioned for zero field broadening but can include different modes of flux motion.

As with the zero field results, MgB_2 will be used as a starting point. The field dependent $(\Delta T_c/T_c)_B$ with the zero-field value of $(\Delta T_c/T_{c0})$ subtracted are shown for many MgB_2 measurements in Figure 9. The solid lines are 3rd order polynomial fits to the data of Canfield¹⁸ for a polycrystalline and Pradhan¹⁹ for a single crystal sample. These two measurements are clearly a good representation of the range of the field dependent MgB_2 data. From Equation 8, the range of observed slopes should vary as the cube root of the zero field broadening, found to be ~ 65 from Table I, which is approximately 4. For different values of B/B_{c2} the ratio of the data of Canfield and Pradhan in Figure 9 vary by values from 3.5-5 in excellent agreement with this expectation.

Figure 10 shows the broadening for all of the H-rich superconductors for those with (a) $T_c < 200$ K and (b) $T_c > 200$ K separated here only for clarity. Most of the H-rich materials have values that lie within the range of the MgB_2 curves. There is a general trend that the slope decreases with higher T_c value. This decrease in the magnetic field dependence is a natural result of Equation 8. However, there still exists a great deal of variation in the slopes of the H-rich data due to different broadening effects. To compare the H-rich samples for all T_c values, the magnetic field data will be rescaled using Equation 8. However, instead of using the sharpest possible zero field broadening Gi , Gi will be replaced by the zero field value of the broadening $(\Delta T_c/T_c)_0$ which should to some extent take into account the intrinsic broadening of the system.

Figure 10(c) shows the $(\Delta T_c/T_c)_B$ data from Figure 10(a) and 10(b) divided by a factor of $((\Delta T_c/T_c)_0)^{1/3}$. The range of slopes now does not exhibit a general T_c dependence and nothing stands out as anomalous. To summarize the results on the transition broadening in H-rich materials:

- The range of $\Delta T_c/T_c$ values for the materials with similar T_c values in zero field can vary greatly (around a factor of 60) for a variety of reasons. This range is independent of the value of T_c and is similar to MgB_2 .
- The rescaled values of the additional broadening $(\Delta T_c/T_c)_B$ in applied fields show a wide variation as do the various values for MgB_2 . The rescaled

H-rich data show the expected transition broadening with applied magnetic field with neither a discernible T_c dependence nor obvious anomalous behavior.

E. Moving to the Clean Region

The H-rich superconductors lie almost entirely outside of the clean limit. As great effort is being put into raising T_c , it is instructive to look at expected behavior from our GLAG scaling into this region. The highest $T_c=288$ K in CSH puts all of the H-superconductors in the region $\tau < 1.24$ which is just slightly into the clean region using our criteria. If T_c is raised higher than 288 K in H-rich systems the GLAG theory would predict the following. (1) The superconducting transition width will rapidly increase. (2) B_{c2} should increase with increasing T_c . A minimum in B_{c2} occurs due to the large increase in ℓ making $\xi = \xi_{GL}$ and $B_{c2} \propto (\xi_{GL})^{-2} \propto m^{*4}$. (3) T_c will increase with an increase in effective mass. $T_c \propto m^{*7/3}$ which is faster than the linear behavior in the dirty limit.

II. CONCLUSIONS

Using the Ginzburg-Landau-Abrikosov-Gorkov (GLAG) theory, many aspects of the superconductivity in all of the hydrogen-rich materials observed to exhibit high-pressure superconductivity can be explained. This includes the following as T_c increases: observation of a maximum in B_{c2} , a break in slope of $T_c(P)$, and decreasing superconducting transition widths. All of the H-rich superconductors follow the GLAG theory's predicted universal behavior regardless of applied pressure with effective mass increasing with T_c being the driving force. This analysis also shows that raising the effective electron mass should continue raising the superconducting transition temperature even higher than room temperature. This should encourage more hydrogen dominant alloys to be synthesized that display larger effective masses and therefore T_c 's at lower densities.

III. ACKNOWLEDGEMENTS

This work supported in part by the U.S. Department of Energy, Office of Basic Energy Sciences under Award Number DE-SC0020303.

IV. APPENDIX A: TABLES

- * andrew.cornelius@unlv.edu
- ¹ C. J. Pickard, I. Errea, and M. I. Eremets, *ANNUAL REVIEW OF CONDENSED MATTER PHYSICS, VOL 11, 2020*, edited by Marchetti, MC and Mackenzie, AP, Annual Review of Condensed Matter Physics, Vol. 11 (2020) pp. 57–76.
 - ² S. Di Cataldo, C. Heil, W. von der Linden, and L. Boeri, *Physical Review B* **104** (2021), [10.1103/PhysRevB.104.L020511](https://doi.org/10.1103/PhysRevB.104.L020511).
 - ³ E. Snider, N. Dasenbrock-Gammon, R. McBride, M. Debessai, H. Vindana, K. Venkatasamy, K. V. Lawler, A. Salamat, and R. P. Dias, *Nature* **586**, 373 (2020).
 - ⁴ M. Tinkham, *Physical Review Letters* **61**, 1658 (1988).
 - ⁵ V. L. Ginzburg, *Uspekhi Fizicheskikh Nauk* **167**, 429 (1997).
 - ⁶ L. P. Gorkov, *Soviet Physics JETP-USSR* **9**, 1364 (1959).
 - ⁷ V. Schmidt, *The Physics of Superconductors: Introduction to Fundamentals and Applications*, 1st ed. (Springer, Berlin, Heidelberg, 1997).
 - ⁸ Y. Li and Y. Gao, *Scientific Reports* **7** (2017), [10.1038/s41598-017-01292-4](https://doi.org/10.1038/s41598-017-01292-4).
 - ⁹ R. Flükiger, D. Uglietti, C. Senatore, and F. Buta, *Cryogenics* **48**, 293 (2008).
 - ¹⁰ C. J. Pickard, I. Errea, and M. I. Eremets, *Annual Review of Condensed Matter Physics* **11**, 57 (2020).
 - ¹¹ T. N. De Silva, *Physical Review B* **104** (2021), [10.1103/PhysRevB.104.024503](https://doi.org/10.1103/PhysRevB.104.024503).
 - ¹² A. P. Drozdov, M. I. Eremets, I. A. Troyan, V. Ksenofontov, and S. I. Shylin, *Nature* **525**, 73 (2015).
 - ¹³ S. Mozaffari, D. Sun, V. S. Minkov, A. P. Drozdov, D. Knyazev, J. B. Betts, M. Einaga, K. Shimizu, M. I. Eremets, L. Balicas, and F. F. Balakirev, *Nature Communications* **10** (2019), [10.1038/s41467-019-10552-y](https://doi.org/10.1038/s41467-019-10552-y).
 - ¹⁴ A. S. Sidorenko, in *Nanoscale Devices - Fundamentals and Applications*, edited by R. Gross, A. Sidorenko, and L. Tagirov (Springer Netherlands) pp. 339–348.
 - ¹⁵ R. A. Ferrell and H. Schmidt, *Physics Letters A* **25**, 544 (1967).
 - ¹⁶ J. E. Hirsch and F. Marsiglio, *Nature* **596**, E9 (2021).
 - ¹⁷ G. Blatter, M. V. Feigel'Man, V. B. Geshkenbein, A. I. Larkin, and V. M. Vinokur, *Reviews of Modern Physics* **66**, 1125 (1994).
 - ¹⁸ P. C. Canfield, S. L. Bud'ko, and D. K. Finnemore, *Physica C-Superconductivity and Its Applications* **385**, 1 (2003).
 - ¹⁹ A. K. Pradhan, Z. X. Shi, M. Tokunaga, T. Tamegai, Y. Takano, K. Togano, H. Kito, and H. Ihara, *Physical Review B* **64** (2001), [10.1103/physrevb.64.212509](https://doi.org/10.1103/physrevb.64.212509).
 - ²⁰ K. H. P. Kim, J. H. Choi, C. U. Jung, P. Chowdhury, H. S. Lee, M. S. Park, H. J. Kim, J. Y. Kim, Z. L. Du, E. M. Choi, M. S. Kim, W. N. Kang, S. I. Lee, G. Y. Sung, and J. Y. Lee, *Physical Review B* **65** (2002), [10.1103/PhysRevB.65.100510](https://doi.org/10.1103/PhysRevB.65.100510).
 - ²¹ C. C. Wang, R. Zeng, X. Xu, and S. X. Dou, *Journal of Applied Physics* **108** (2010), [10.1063/1.3488631](https://doi.org/10.1063/1.3488631).
 - ²² V. V. Derevyanko, M. S. Sungurov, T. V. Sukhareva, V. A. Finkel', and Y. N. Shakhov, *Physics of the Solid State* **59**, 229 (2017).
 - ²³ K. Zhang, L.-L. Ding, C.-G. Zhuang, L.-P. Chen, C. Chen, and Q.-R. Feng, *physica status solidi (a)* **203**, 2463 (2006).
 - ²⁴ S. Altin, M. A. Aksan, Z. D. Yakinci, M. Özabaci, Y. Balci, and M. E. Yakinci, *Journal of Physics: Conference Series* **153**, 012001 (2009).
 - ²⁵ E. Altin, F. Kurt, S. Altin, M. E. Yakinci, and Z. D. Yakinci, *Current Applied Physics* **14**, 245 (2014).
 - ²⁶ S. Mizutani, A. Yamamoto, J.-i. Shimoyama, H. Ogino, and K. Kishio, *Superconductor Science and Technology* **27**, 114001 (2014).
 - ²⁷ W. N. Kang, H.-J. Kim, E.-M. Choi, K. H. P. Kim, and S.-I. Lee, *Physica C: Superconductivity* **378-381**, 1246 (2002).
 - ²⁸ W. Chen, D. Semenov, X. Huang, H. Shu, X. Li, D. Duan, T. Cui, and A. Oganov, *Physical Review Letters* **127** (2021), [10.1103/physrevlett.127.117001](https://doi.org/10.1103/physrevlett.127.117001).
 - ²⁹ I. A. Troyan, D. V. Semenov, A. G. Kvashnin, A. V. Sadakov, O. A. Sobolevskiy, V. M. Pudalov, A. G. Ivanova, V. B. Prakapenka, E. Greenberg, A. G. Gavriliuk, I. S. Lyubutin, V. V. Struzhkin, A. Bergara, I. Errea, R. Bianco, M. Calandra, F. Mauri, L. Monacelli, R. Akashi, and A. R. Oganov, *Advanced Materials* **33**, 2006832 (2021).
 - ³⁰ A. P. Drozdov, P. P. Kong, V. S. Minkov, S. P. Besedin, M. A. Kuzovnikov, S. Mozaffari, L. Balicas, F. F. Balakirev, D. E. Graf, V. B. Prakapenka, E. Greenberg, D. A. Knyazev, M. Tkacz, and M. I. Eremets, *Nature* **569**, 528 (2019).
 - ³¹ M. Somayazulu, M. Ahart, A. K. Mishra, Z. M. Geballe, M. Baldini, Y. Meng, V. V. Struzhkin, and R. J. Hemley, *Physical Review Letters* **122** (2019), [10.1103/physrevlett.122.027001](https://doi.org/10.1103/physrevlett.122.027001).
 - ³² F. Hong, L. Yang, P. Shan, P. Yang, Z. Liu, J. Sun, Y. Yin, X. Yu, J. Cheng, and Z. Zhao, *Chinese Physics Letters* **37**, 107401 (2020).
 - ³³ F. Hong, P. F. Shan, L. X. Yang, B. B. Yue, P. T. Yang, Z. Y. Liu, J. P. Sun, J. H. Dai, H. Yu, Y. Y. Yin, X. H. Yu, J. G. Cheng, and Z. X. Zhao, *arXiv pre-print server* (2021), [None arxiv:2101.02846](https://arxiv.org/abs/2101.02846).
 - ³⁴ D. V. Semenov, I. A. Troyan, A. G. Ivanova, A. G. Kvashnin, I. A. Kruglov, M. Hanfland, A. V. Sadakov, O. A. Sobolevskiy, K. S. Pervakov, I. S. Lyubutin, K. V. Glazyrin, N. Giordano, D. N. Karimov, A. L. Vasiliev, R. Akashi, V. M. Pudalov, and A. R. Oganov, *Materials Today* (2021), <https://doi.org/10.1016/j.mattod.2021.03.025>.
 - ³⁵ D. V. Semenov, A. G. Kvashnin, A. G. Ivanova, V. Svitlyk, V. Y. Fominski, A. V. Sadakov, O. A. Sobolevskiy, V. M. Pudalov, I. A. Troyan, and A. R. Oganov, *Materials Today* **33**, 36 (2020).
 - ³⁶ A. P. Drozdov, M. Eremets, and I. Troyan, “Superconductivity above 100 k in ph3 at high pressures,” (2015).
 - ³⁷ E. Snider, N. Dasenbrock-Gammon, R. McBride, X. Wang, N. Meyers, K. V. Lawler, E. Zurek, A. Salamat, and R. P. Dias, *Physical Review Letters* **126** (2021), [10.1103/physrevlett.126.117003](https://doi.org/10.1103/physrevlett.126.117003).
 - ³⁸ L. Ma, K. Wang, Y. Xie, X. Yang, Y. Wang, M. Zhou, H. Liu, G. Liu, H. Wang, and Y. Ma, *arXiv pre-print server* (2021), [None arxiv:2103.16282](https://arxiv.org/abs/2103.16282).

	H ₃ S	LaH ₁₀
P (GPa)	155	130
T_c (K)	196	233
$\tau = T_c/T_{c0}$	0.84	1.00
WHH B_{c2} (T)	88	222
ξ (nm) from B_{c2}	1.9	1.2
ℓ (nm) from transport	1.3	4.0
ξ_{AV} (nm) from ξ and ℓ	0.97	1.0
ξ_{GL} (nm) from ξ and ℓ	3.8	1.4
B_{c1} (T)	1.7-2.5	0.8-3.0
κ from B_{c1} and B_{c2}	5.5-7.1	9.0-20.5
$\lambda_L = \kappa\xi_{AV}$ (nm)	5.3-6.9	9.0-20.5

TABLE I. Ginzburg-Landau-Abrikosov-Gorkov (GLAG) parameters for H₃S and LaH₁₀ at the the given pressures. $T_c = 233K$ is the value for the superconducting transition temperature in H-rich superconductors where B_{c2} reaches its maximum value.

Sample Info	T_c (K)	ΔT_c (K)	$\Delta T_c/T_c$	Reference
Poly	40.2	0.49	0.012	Canfield ¹⁸
Single B	36.0	0.32	0.0089	Kim ²⁰
Single B c	36.0	0.32	0.0089	Kim ²⁰
Many doped MgB ₂ Poly**	37	0.31	0.0084	Wang ²¹
Poly	38.8	0.20	0.0052	Derevyanko ²²
Poly #1	37.5	0.36	0.0096	Pradhan ¹⁹
Poly #2	38.0	0.90	0.023	Pradhan ¹⁹
Single B ab	38.2	0.69	0.018	Pradhan ¹⁹
Single B c	38.2	0.69	0.018	Pradhan ¹⁹
TFilm	36.2	0.76	0.021	Sidorenko ¹⁴
TFilm	40.2	0.16	0.0040	Zhang ²³
TFilm 600 C	36.5	9.5	0.26	Altin ²⁴
TFilm 900 C	36.5	2.7	0.074	Altin ²⁴
tFilm A	36.2	1.9	0.054	Altin ²⁵
tFilm B	33.3	1.3	0.038	Altin ²⁵
tFilm C	33.4	3.1	0.091	Altin ²⁵
tFilm D	31.2	5.9	0.19	Altin ²⁵
Poly 1h sinter	38.5	0.59	0.015	Mizutani ²⁶
Poly 6h sinter	38.4	0.57	0.014	Mizutani ²⁶
Poly 24h sinter	38.4	0.48	0.013	Mizutani ²⁶
tFilm	39.2	0.21	0.0054	Kang ²⁷

TABLE II. Superconducting properties of MgB₂ samples from the literature having magnetic field measurements. For sample info: Poly and Single mean polycrystalline and single crystal respectively. tFilm and TFilm mean thin and thick film respectively. Any other text in the Sample Info column is descriptive information from the authors. **Values are for 8 pure and doped polycrystalline samples.

System	T_c (K)	P (GPa)	ΔT_c (K)	$\Delta T_c/T_c$	$B_{c2}(T)$ (GL/WHH)	Reference
CeH ₉	49	88	12.2	0.24	24.7/33.5	Chen ²⁸
	101	139	6.4	0.063	21.2/28.6	
	63	100	4.9	0.078	26.0/35.6	
YH _x	224	166	1.2	0.0055	N/A	Troyan ²⁹
	218	165	7.2	0.033	N/A	
	210	183	1.5	0.0070	116/158	
H ₃ S	51	155	31.9	0.64	25/33*	Drozdov ⁷
	181	195	17.3	0.096	72/85*	
	21	107	9.7	0.46		
	71	177	9.9	0.14		
LaH ₁₀	246	150	7.4	0.030	115/160*	Drozdov ³⁰
	112	150	4.2	0.038		
	73	150	4.8	0.066		
CSH	280	272	18.5	0.068		Snider ³
	188	210	0.7	0.0032	48/66	
	288	267	0.28	0.00010	62/85	
LaH ₁₀	248	188	2.9	0.012	N/A	Somayazulu ³¹
LaH ₁₀	233	165	5.8	0.025	176/222	Hong ³²
	74	165	78.8	1.06	N/A	
SnH _x	75	200	2.0	0.026	11.2/9.4	Hong ³³
(La,Y)H ₁₀	249	186	11.3	0.046	100/135	Semenok ³⁴
	243	191	7.76	0.032	N/A	
	247	183	11.7	0.048	N/A	
ThH _x	153	170	1.75	0.012	44/63	Semenok ³⁵
	159	174	2.51	0.016	N/A	
	146	170	6.1	0.038	N/A	
PH ₃	100	207	13.6	0.137	N/A	Drozdov ³⁶
	79	180	10.8	0.138	N/A	
	40	117	6.1	0.152	N/A	
YH _x	262	182	7.9	0.030	N/A	Snider ³⁷
	253	177	8.1	0.032	102/117*	
	244	144	12.4	0.047	N/A	
CaH ₆	117	139	23.2	0.198	N/A	Ma ³⁸
	179	129	9.7	0.054	N/A	
	213	172	1.5	0.0070	131/180	
	214	178	5.4	0.025	142/203	

TABLE III. Superconducting parameters for H-rich materials at high pressure. The B_{c2} values were taken or calculated from the referenced publication. GL/WHH refer to the Ginzburg-Landau (GL) and Werthamer-Helfand-Hohenberg (WHH) formalisms for estimating the zero-temperature value $B_{c2} = B_{c2}(0)$. * Value was estimated from the published data for the WHH formalism using $B_{c2} = -0.69T_c B_{c2}'$ where B_{c2}' is the temperature derivative of B_{c2} at T_c .